AAPS PharmSciTech, Vol. 19, No. 7, October 2018 (© 2018)
DOI: 10.1208/s12249-018-1137-6

Research Article

Optimization of Ciprofloxacin Hydrochloride Spray-Dried Microparticles for Pulmonary Delivery Using Design of Experiments

Mariela Razuc,[1,2,4] Juliana Piña,[2,3] and María V. Ramírez-Rigo[1,2]

Received 17 May 2018; accepted 27 July 2018; published online 13 August 2018

Abstract. Ciprofloxacin is a broad-spectrum antibiotic for treatment of pulmonary diseases such as chronic obstructive pulmonary disease and cystic fibrosis. The purpose of this work was to rationally study the spray drying of ciprofloxacin in order to identify the formulation and operating conditions that lead to a product with aerodynamic properties appropriate for dry powder inhalation. A 2^{4-1} fractional factorial design was applied to investigate the effect of selected variables (*i.e.*, ciprofloxacin hydrochloride (CIP) concentration, drying air inlet temperature, feed flow rate, and atomization air flow rate) on several product and process parameters (*i.e.*, particle size, aerodynamic diameter, moisture content, densities, porosity, powder flowability, outlet temperature, and process yield) and to determine an optimal condition. The studied factors had a significant effect on the evaluated responses (higher p value 0.0017), except for the moisture content (p value >0.05). The optimal formulation and operating conditions were as follows: CIP concentration 10 mg/mL, drying air inlet temperature 110°C, feed volumetric flow rate 3.0 mL/min, and atomization air volumetric flow rate 473 L/h. The product obtained under this set had a particle size that guarantees access to the lung, a moisture content acceptable for dry powder inhalation, fair flowability, and high process yield. The PDRX and SEM analysis of the optimal product showed a crystalline structure and round and dimpled particles. Moreover, the product was obtained by a simple and green spray drying method.

KEYWORDS: ciprofloxacin hydrochloride; dry powder inhaler; spray drying; design of experiments; green process.

INTRODUCTION

Chronic obstructive pulmonary disease (COPD) is the fourth leading cause of death in the USA and the sixth leading cause worldwide (1). It is predicted to be the third most common cause of death and chronic disability in the world by 2030 (2). Viral and bacterial infections are the major cause of exacerbations of COPD (3).

On the other hand, cystic fibrosis (*CF*) is a complex genetic disease affecting many organs, being lung damage secondary to chronic infection the main determinant of morbidity and mortality in individuals with this disease (4). Therefore, repeated and intensive antibiotic therapies are required to maintain lung function and quality of life and to reduce exacerbations in infected patients (5).

Antibiotic therapies of these diseases are mainly aimed at eradicating *Pseudomonas aeruginosa*, which is the major bacterial pathogen in *CF* (5), and the cause of severe exacerbations of COPD (6). In these sense, ciprofloxacin has produced good clinical response rates in adults with acute exacerbations of cystic fibrosis (7). Moreover, the World Health Organization indicates that the treatment of *Pseudomonas aeruginosa* infection in *CF* is one of the most important uses of ciprofloxacin (8). On the other hand, ciprofloxacin is the antibiotic of choice for the treatment of patients with severe exacerbations of COPD (9).

Delivery of antibiotics *via* the pulmonary tract to treat respiratory infections is advantageous over more conventional routes (as the oral one) since the lungs are directly targeted. Targeted delivery allows reducing the therapeutic dose, leading to a decrease in potential drug resistance build-up and a reduction in side effects, often associated with high oral doses (10,11). Dry powder inhalation (DPI) formulations

Electronic supplementary material The online version of this article (https://doi.org/10.1208/s12249-018-1137-6) contains supplementary material, which is available to authorized users.

[1] Departamento de Biología, Bioquímica y Farmacia, Universidad Nacional del Sur (UNS), Bahía Blanca, Argentina.
[2] Planta Piloto de Ingeniería Química (PLAPIQUI), UNS-CONICET, Camino La Carrindanga Km 7 (8000), Bahía Blanca, Argentina.
[3] Departamento de Ingeniería Química, UNS, Bahía Blanca, Argentina.
[4] To whom correspondence should be addressed. (e–mail: mariela.razuc@uns.edu.ar)

incorporate a powder containing the drug as micron-sized particles, which upon inhalation is aerosolized from a device to be deposited in the lower respiratory tract. The particle size of the drug to be delivered is critical for its efficient deposition in the lower airways. Particles with diameters between 1 and 5 μm are able to access deep lungs. However, particles smaller than 1 μm are exhaled during normal tidal breathings while those larger than 5 μm are deposited in the upper airways with a vigorously mucociliary clearance (12). Therefore, producing particles with the required size and specific structures is challenging for DPI use. Dry powder systems have many advantages over liquid nebulizer systems. DPI-based formulations are in solid state and therefore less susceptible to chemical degradation. Furthermore, the devices are generally less expensive, require little maintenance, and can be manufactured in a disposable form (13). Moreover, DPIs are able to administrate high amount of drugs, being relevant in antibiotic therapies. Hence, there is a growing interest in developing DPI formulations with a minimal quantity of excipients, and, if it is possible "carrier-free" (*i.e.*, without excipients) (14).

Dry powder inhalation can be prepared through different techniques, such as milling, supercritical fluid technology, crystallization by ultrasonic precipitation, and spray drying (SD) (15). Particularly, spray drying is a simple, continuous, cost-effective, reproducible, and scalable process (16). This technique allows changing certain conditions with the purpose of obtaining products with specific characteristics. Adjustable parameters of the SD technique are related with the process, the liquid feed and the equipment. The main ones are the following: flow rate, inlet temperature and type of drying gas, flow rate, concentration, viscosity, density, surface tension and solvent boiling point of the liquid feed, co-current, counter-current or mixed flow, and atomizer geometry (16). Changes in theses parameters lead to variations in process yield, particle size and morphology, crystalline state, moisture content and density, among others. (17,18).

There are a series of articles in the open literature about the spray drying of ciprofloxacin for DPI (13,19–28). Most of the developed formulations include high proportions (> 50% *w*/*w*) of different types of excipients. This fact is particularly important in antibiotic administration where high doses of drugs are necessary. To the best of our knowledge, Zhao *et al.* (25) are the unique ones who developed a DPI containing only ciprofloxacin. In this case, the product is obtained by combination of reactive precipitation and anti-solvent precipitation, followed by the SD process. Cotabarren *et al.* (26) combined experimentation of spray drying and modeling with the purpose of providing a simulation tool for the rational design of inhalatory particles and used ciprofloxacin as a model inhalable compound. A few works that have developed DPI formulations of CIP in combination with others drugs or excipients compare the corresponding mixtures with a DPI containing only CIP (13,19,23,24). However, in all of them, the performance of the aerodynamic behavior is not high enough or the production process includes several steps with the use of organic solvents. It is important to note that none of these articles addressed the optimization of the spray drying process.

Optimizing methodologies for green chemical processing are in line with the purpose of reducing the environmental effect of the pharmaceutical industry. In 2005, the American Chemical Society (ACS), the Green Chemistry Institute (GCI), and several leading global pharmaceutical corporations developed the ACS GCI Pharmaceutical Roundtable (29). The Roundtable's mission is to catalyze the implementation of green chemistry and green engineering in the global pharmaceutical industry. It is important to note that the implementation of these principles also brings economic benefits.

In this context, the aim of this work is to find the optimal formulation and operating conditions for the spray drying of ciprofloxacin aqueous solutions in order to produce, through a single step and a green method, particles with aerodynamic diameters appropriate for a DPI. By means of a 2^{4-1} fractional factorial design, the effect of selected factors (ciprofloxacin hydrochloride concentration, drying air inlet temperature, feed flow rate, and atomization air flow rate) on different key product and process parameters (particle size and morphology, aerodynamic diameter, moisture content, powder flowability, outlet temperature, and process yield) was analyzed. A statistical model was fitted for each response as a function of the independent factors. Finally, the models were combined in order to find an optimum set of conditions that improves the product and process responses simultaneously. Complementarily, an environmental analysis based on the 12 principle of the Green Chemistry was performed.

MATERIALS AND METHODS

Materials

Ciprofloxacin hydrochloride (CIP) and lactose monohydrate, pharmaceutical grade, were purchased from Parafarm, Saporiti (Buenos Aires, Argentina). Lactose was sieved by using a 100 ASTM mesh (particle size bigger than 149 μm). Glycerin was purchased from Anedra (Buenos Aires, Argentina). During the whole experimental process, bi-distilled water was used.

Preparation and Characterization of the SD Feed Solutions

CIP feed solutions (at two different concentrations, 10 mg/mL and 50 mg/mL) were prepared just before the SD process, by mixing the raw CIP powder with water at 40°C. The mass of CIP in the solutions was kept constant at 2.5 g; thus, the CIP concentration varied according to the amount of water used. The kinematic viscosity, density, and surface tension were measured and reported in a previous work (26). Generally, these properties affect the quality of the SD products and the process performance. However, these properties were very similar to those of pure water. The values obtained were in the range of 1.4150–1.5791 (mm^2/s) for the kinematic viscosity, 0.9970–1.0128 (g/mL) for the density, and 63.0–69.6 (mV/m) for the surface tension.

Spray Drying Process

The CIP aqueous solutions were dried by using a Mini Spray Dryer B-290, BÜCHI (Flawil, Switzerland) in open loop mode, equipped with a *high-performance cyclone*. A standard 0.5-mm two-fluid nozzle was used. The drying air volumetric flow rate was at 100% aspiration (about 35–38 m^3/h) for all the performed experiments. The remaining process parameters were set by the factorial design study outlined in the "Experimental Design" section. The process yield was calculated as the ratio between the mass of product obtained by SD and the mass of the feed solid content, being all the values expressed on a dry-matter basis.

After the spray drying, the different parts of the equipment (dryer chamber, cyclone, and collector) were washed with distillated water. The obtained solutions were then measured at 274.5 nm in a UV-Vis spectrophotometer (Shimadzu UV-160, Kyoto, Japan) in order to determine the amount of CIP found in each part of the equipment. The recovery percentage was calculated as the sum of process yield, dryer chamber percentage, cyclone percentage, and collector percentage (powder remaining after product collection).

Experimental Design

An experimental design was performed to identify the critical factors in CIP spray drying and to evaluate the effect of these factors on key product attributes and process performance. A 2^{4-1} fractional factorial design was used. The statistical analysis was carried out by means of the Design Expert software (version 7.0.0). Based on results of preliminary trials and those reported in bibliography (19,20,24–28,30), the selected factors and levels were as follows: (A) CIP concentration, 10 mg/mL (−) and 50 mg/mL (+); (B) drying air inlet temperature, 110°C (−) and 180°C (+); (C) feed volumetric flow rate, 3 mL/min (−) and 6 mL/min (+); and (D) atomization air volumetric flow rate, 473 L/h (−) and 670 L/h (+). All the experimental runs were performed in duplicate and in a randomized manner to eliminate any unknown possible sources of bias (31). The purpose of replication was to decrease experimental error and increase the precision of the experiments.

It is important to clarify that this design represents a resolution IV design. In this case, each main effect (A, B, C, and D) is aliased with a three-factor interaction (*e.g.*, the A factor is aliased with the BCD interaction). Assuming that three-factor interactions are improbable, it is possible to estimate the main effects from this design. On the contrary, all two-factor interactions are aliased with each other. Thus, two-factor interactions cannot be concluded from this design (*e.g.*, the AB interaction is aliased with the CD interaction) (32).

Characterization of the SD Powder

Moisture Content

The moisture content (MC) of the SD powders was determined by using a halogen moisture analyzer (MB45, Ohaus, Pine Brook, USA). Around 500 mg of sample were heated up to 80°C until the weight change was less than 1 mg in 90 s. These determinations were carried out immediately after the spray drying process.

Particle Size Analysis

The particle size distribution of the SD powders was determined by laser diffraction (LA 950V2, Horiba, Kyoto, Japan). The powders were dispersed in lactose (lactose:sample 4:1) to improve the powder flow from the feed hopper to the measuring cell (33). Average particle size is expressed as median volume diameter (D_{50}) and the distribution width is reported as span (Eq. (1)).

$$\text{Span} = \frac{(D_{90} - D_{10})}{D_{50}} \tag{1}$$

where D_{10}, D_{50}, and D_{90} correspond to the diameters below which the 10, 50, or 90% of the population lies. A distribution can be considered relatively narrow if the span value is less than 2 (33). In addition, the percentage of particles lower than 5 μm was calculated for all SD products.

Skeletal, Bulk, and Tap Density Determination

The sample or skeletal density (δ_s) of the SD powders was determined by nitrogen adsorption (Nova 1200e, Quantachrome Instruments, FL, USA). One gram sample was placed in a precalibrated cell and its volume was determined by nitrogen intrusion. The sample density was calculated as the solid mass divided by the volume of the particles excluding the open pores.

In addition, the bulk density (δ_{bulk}), tap density (δ_{tap}), and Carr's index (CI) were calculated. The δ_{bulk} was determined by measuring the volume of a known mass of powder (without tapping) into a 10-cm^3 graduated cylinder. On the other side, the δ_{tap} was estimated by tapping the cylinder until no measurable change in volume was noticed. The powder flowability was assessed by the Carr's (compressibility) index. This index was calculated from the bulk and tap densities, as it is shown in Eq. (2).

$$\text{CI} = 100\frac{(\delta_{tap} - \delta_{bulk})}{\delta_{tap}} \tag{2}$$

The United States Pharmacopeia gives a scale of flowability and CI. In this scale, the flow of a powder can be considered excellent (< 10), good (11–15), fair (16–20), passable (21–25), poor (26–31), very poor (32–37) or very, very poor (> 38) according to the calculated CI (34).

Estimated Aerodynamic Diameter

For each SD powder, the aerodynamic diameter (D_{aer}) was estimated from its D_{50} and the tap and skeletal densities, as follows Eqs. (3) and (4) (35):

$$D_{aer1} = D_{50}\sqrt{\delta_s} \quad (3)$$

$$D_{aer2} = D_{50}\sqrt{\delta_{bulk}} \quad (4)$$

The particle density (δ_p) is equal to the δ_s for non-porous particles. In the case of porous or void particles, the δ_s is higher than the δ_p. Therefore, the D_{aer} calculated with δ_s will be overestimated (Eq. (3)) (36). On the other side, if the δ_{bulk} is used in Eq. (4) instead of δ_p, the aerodynamic diameter will be underestimated because δ_{bulk} is always lower than the particle density. Indeed, the particle density will be between the skeletal density and the bulk density.

Scanning Electron Microscopy

The morphology of the SD and raw particles was examined by scanning electron microscopy using an EVO 40-XVP LEO scanning electron microscope (Oberchoken, Germany) at 10 kV. Prior to imaging, the samples were dispersed onto carbon sticky tabs and metalized with gold using a sputter coater (PELCO 91000, TellPella, Canada).

Powder X-ray Diffraction

With the purpose of knowing the solid state, crystalline or amorphous, of the obtained products, a PXRD analysis was carried out. Sample diffractograms were recorded between 5° and 60° on the (2θ) scale (Rigaku, Geigerfleck, Tokyo, Japan), using an anodic cupper tube with a monochromator (35 kV and 15 mA). Angle and time steps of 0.04° and 0.8 s were selected, respectively.

Experimental Aerodynamic Behavior

A Next Generation Impactor (NGI, Coplay, Nottingham, UK) equipped with an induction port (IP) was used to determinate the aerodynamic performance of the optimal SD product. The NGI is constituted by a seven-stage inertial impactor that separates the powder into different ranges of aerodynamic diameters and, as a final stage, by a micro-orifice collector (MOC) (37). A RS01 inhaler (Plastiape) containing the SD product in a capsule was connected to the IP *via* a mouthpiece adapter (MA). Previous to the powder aerosolization, the NGI stages were pre-coated with glycerin to avoid particle re-entrainment.

A three-size gelatin capsule was filled with 37.9 (± 0.1) mg of ciprofloxacin hydrochloride SD powder, corresponding to 32.5 mg ciprofloxacin. Stass *et al.* (38) reported that 32.5 mg of CIP DPI are safe and well tolerated in healthy male adults. In addition, this dose significantly prolonged time to first exacerbation and reduced exacerbation frequency in non-cystic fibrosis bronchiectasis (39).

The NGI was operated at 60 L/min for 4 s, with a pressure drop of 4 kPa. The aerodynamic cut-off diameters of each NGI stage were calculated as described by Marple *et al.* (34,40).

After powder aerosolization, the NGI stages, inhaler, IP, and MA were washed with water. The determination of CIP in the resulting solutions was carried out by UV spectrophotometry at 274.5 nm (Shimadzu UV-160, Kyoto, Japan). Experiments were done by triplicate. The emitted fraction (EF), the fine particle fraction (FPF), and respirable fraction (RF) were calculated as follows (41):

$$EF\% = \frac{\text{mass of drug deposited on induction port and all the NGI stages}}{\text{total drug recovered}} \times 100 \quad (5)$$

$$FPF\% = \frac{\text{mass of drug deposited on stages 3–7 and MOC}}{\text{mass of drug deposited on induction port and all the NGI stages}} \times 100 \quad (6)$$

$$RF\% = \frac{\text{mass of drug deposited on stages 3–7 and MOC}}{\text{total drug recovered}} \times 100 \quad (7)$$

The mass median aerodynamic diameter (MMAD) and the geometric standard deviation (GSD) were also determined according to USP for apparatus 5 (34). The GSD represents the spread of the aerodynamic particle size distribution. It was calculated using Eq. (8).

$$GSD = \left(\frac{D_{84}}{D_{16}}\right)^{1/2} \quad (8)$$

where D_{16} and D_{84} are the diameters at which 16 and 84% of the drug mass are recovered from the NGI 1–7 stages and MOC. The corresponding values were calculated using a fitted polynomial equation that satisfactorily fit the volume passing cumulative distribution.

RESULTS AND DISCUSSION

Statistical Evaluation of the Experimental Design

Table I shows the experiment design matrix together with the results obtained for the studied responses. The results were used to determine the fitted model equations for the responses (Table II). The factors and factor interactions included in each equation were significant for the model at the 95% confidence level, unless otherwise indicated. No significant factors are noted with a superscript *n*. Nevertheless, these factors were included in the corresponding models to assure obtaining hierarchical models (32). Models were considered adequate when the following criteria were satisfied: no lack of fit (p value > 0.05), regression test (p value < 0.05), high and similar goodness of fit (R^2), and prediction estimates (adjusted R^2), which are ideally above 0.9 and 0.7, respectively (42). Previous transformation of the data was not required.

Process Yield and CIP Recovery in Different Parts of the Spray Dryer

Table I shows the yield achieved for each experiment. The lowest and highest yields were 55.9 and 87.1%, respectively. Except in just a few experiments, the yields were greater than or equal to 70% being this value more than acceptable for lab-scale spray dryers. The ANOVA analysis results for the model are shown in Table II. The low p value of the model (< 0.0001) and the non-significant lack of fit (p value 0.2037) proved the applicability of the predictive model. In addition, the R^2 and predicted R^2 values were higher than 0.9000 and the observed values *vs.* predicted values plots indicated a reasonable good fit (Fig. 1).

Table II shows that the A and D factors, as well as the AD interaction had a significant effect on the process yield. As was previously mentioned, in a resolution IV design, the two-factor interactions are aliased with each other ("Experimental Design" section). In this case, the AD interaction is aliased with the BC interaction. Considering that the significant factors in this model are A and D, it can be concluded that the significant AD interaction corresponds to the AD interaction and it is not aliased with BC. As expected, the CIP concentration of the feed solution (A factor) had a positive effect on the process yield (17). In this sense, the highest process yields were obtained for the highest tested CIP concentration (*i.e.*, 50 mg/mL). On the other side, the atomization air volumetric flow rate (D factor) showed a negative effect on the process yield. The same can be concluded from the 3D plot of the process yield showed in Fig. 2. As it can be seen, the yield is high and decreases as the CIP concentration decreases and the atomization air volumetric flow rate increases.

In order to know the destination of the drug not recovered as product, a relationship analysis over the drug percentage in different parts of the equipment was carried out. Table S.I shows the drug percentage obtained in each part for every point of the experimental design. For the runs with low process yield (*i.e.*, runs 1, 4, 7, and 9), the recovery in the cyclone was high. This relationship is also shown in Fig. S.1.B, where the process yield decreases as the cyclone percentage increases. On the other side, no relationship was observed between the yield and the chamber percentage (Table S.I and Figure S.1.A). However, the runs with the low yield present low chamber percentages. Therefore, sticking on the chamber walls is not the cause of the reduction in the process yield, being mainly affected by the percentage of drug stuck on the cyclone walls.

Outlet Temperature

The outlet temperature (T_{out}) was monitored during each SD run. The values showed in Table I are averages between the upper and lower registered temperature. In all cases, these changes were below 3°C. The outlet temperature varied between 44.5 and 95.0°C. The statistical model was significant with a p value < 0.0001 and a LOF higher than 0.0500. The R^2 as well as R^2 predicted was above 0.9000. In addition, Fig. 1 shows adequate agreement between experimental and predicted data.

Within the studied limits, the CIP concentration (factor A) did not affect the outlet temperature. The remaining factors B (p value < 0.0001), C (p value 0.0001), and D (p value 0.0181) had significant effects on T_{out}. As expected, the outlet temperature increased as the inlet temperature increased and as the feed and atomization air flow rates decreased (17). The effects of the most significant factors (B and C) on T_{out} are shown in Fig. 2.

It has been demonstrated that ciprofloxacin hydrochloride dehydrates at 167–170°C, melts at 326–327°C, and decomposes at 350°C (43,44). In the present work, the highest

Table I. Experimental Matrix According to 2^{4-1} Factorial Design and Studied Responses

Run	A	B	C	D	T_{out}* (°C)	MC* (%)	Yield (%)	Recovery (%)	D_{50} (μm)	Span	PPB_5 (%)	δ_s* (g/mL)	δ_{bulk} (g/mL)	δ_{tap} (g/mL)	ϕ	CI	D_{aer1} (μm)	D_{aer2} (μm)
1	−	−	+	+	44.5	2.84	57.6	91.3	7.7	1.4	19.3	1.234	0.341	0.450	0.723	24	8.5	4.5
2	+	−	−	+	51.5	3.83	86.0	93.6	4.4	1.2	60.2	1.274	0.318	0.400	0.747	24	5.0	2.5
3	+	−	+	−	47.5	2.13	79.8	95.8	7.7	0.9	13.1	1.243	0.363	0.513	0.708	29	8.6	4.6
4	−	+	−	+	82.5	2.90	55.9	85.6	5.7	1.3	38.6	1.259	0.374	0.494	0.703	23	6.4	3.5
5	−	+	+	−	80.5	1.21	83.1	94.3	6.3	1.1	29.8	1.220	0.282	0.432	0.769	35	7.0	3.4
6	−	−	−	−	60.0	2.09	80.7	94.6	4.9	1.1	50.1	1.231	0.384	0.448	0.688	14	5.5	3.1
7	−	+	−	+	92.5	3.05	59.1	90.4	5.6	2.0	42.5	1.256	0.384	0.467	0.694	18	6.2	3.4
8	+	−	−	+	60.5	2.46	87.1	94.0	5.4	1.1	43.3	1.289	0.317	0.449	0.741	24	6.1	3.0
9	−	−	+	+	47.0	4.57	62.7	93.4	6.9	1.4	26.4	1.204	0.343	0.433	0.715	21	7.6	4.0
10	−	−	−	−	61.5	2.08	83.4	95.5	4.6	0.9	58.7	1.218	0.361	0.486	0.683	19	5.0	2.7
11	+	−	+	−	47.5	2.84	74.8	95.5	7.9	1.0	13.8	1.232	0.348	0.492	0.718	29	8.8	4.7
12	−	+	+	−	87.5	2.54	79.3	95.0	6.8	1.0	22.8	1.220	0.318	0.463	0.740	31	7.5	3.8
13	+	+	−	−	95.0	2.01	83.7	95.8	6.9	1.0	23.1	1.257	0.309	0.480	0.754	36	7.7	3.8
14	+	+	+	+	80.5	1.99	84.1	93.9	7.2	1.1	19.8	1.230	0.312	0.402	0.758	26	8.0	4.0
15	+	+	+	+	68.0	3.79	83.9	94.0	7.6	1.1	18.0	1.203	0.296	0.419	0.754	29	8.4	4.2
16	+	+	−	−	94.0	1.73	81.5	95.9	7.5	1.0	16.0	1.246	0.300	0.457	0.759	34	8.3	4.1

T_{out} outlet temperature, MC moisture content, D_{50} median volume diameter, PPB_5 percentage of particles below 5 μm, δ_s skeletal density, δ_{bulk} bulk density, δ_{tap} tap density, ϕ porosity, CI Carr's index, D_{aer1} aerodynamic diameter calculated with δ_s, D_{aer2} aerodynamic diameter calculated with δ_{bulk}. *Cotabarren *et al.* [26], reported the mean values between replicates

Table II. Coefficients of the Quadratic Equations (in Terms of Coded Factors) Linking the Spray Drying Parameters with the Studied Responses. Results of the ANOVA Analysis

Run	Aliased	T_{out} (°C)	Yield (%)	D_{50} (μm)	PPB_5 (%)	δ_s (g/mL)	δ_{bulk} (g/mL)	ϕ	CI	D_{aer1} (μm)	D_{aer2} (μm)
Transform		–	–	–	–	–	–	–	–	–	–
Intercept		+68.78	+76.42	+6.44	+30.98	+1.24	+0.33	+0.73	+26.05	+7.16	+3.71
A	BCD	–	+6.19	+0.38	−5.07	+0.008	−0.014	+0.014	+2.99	+0.45	+0.15
B	ACD	+16.28	–	+0.26	−4.65	−0.002[c]	−0.013	+0.013	+2.97	+0.28	–
C	ABD	−5.91	–	+0.83	−10.61	−0.015	−0.009	+0.007	+2.08	+0.89	+0.44
D	ABC	−2.91	−4.37	−0.13[c]	+2.54[c]	–	+0.001[c]	+0.0009[c]	−2.42	−0.14[c]	−0.062[c]
AB	CD	–	–	+0.22	–	−0.011	–	–	–	–	–
AC	BD	–	–	–	–	–	+0.018	−0.015	−2.60	–	–
AD	BC	–	+7.03	−0.54	+6.87	–	−0.011	+0.006	–	−0.60	−0.38
Model (p value)[a]		<0.0001	<0.0001	<0.0001	<0.0001	0.0017	0.0003	<0.0001	<0.0001	<0.0001	<0.0001
LOF (p value)[b]		0.8376	0.2037	0.7326	0.3529	0.1847	0.2864	0.6895	0.3070	0.2036	0.2287
R^2		0.9550	0.9517	0.9425	0.9088	0.7686	0.9076	0.9482	0.9094	0.9087	0.8884
Predicted R^2		0.9200	0.9141	0.8181	0.7665	0.5105	0.7079	0.8362	0.7681	0.7663	0.7638

T_{out} outlet temperature, MC moisture content, D_{50} median volume diameter, PPB_5 percentage of particles below 5 μm, δ_s skeletal density, δ_{bulk} bulk density; δ_{tap} tap density, ϕ porosity, CI Carr's index, D_{aer1} aerodynamic diameter calculated with δ_s, D_{aer2} aerodynamic diameter calculated with δ_{bulk}

[a] Reference value for good model < 0.05

[b] Reference value for good model > 0.05

[c] Not significant

inlet and outlet temperatures were 180 and 95°C, respectively. These thermal levels are well below the melting and decomposition temperatures. However, a dehydration process could happen for the experimental runs performed at an inlet temperature of 180°C (above the dehydrate temperature, 170°C).

Moisture Content

The moisture content (MC) of the SD powders was between 1.21 and 4.57% (Table I). Low MC values (< 5%) are required in spray-dried products to ensure good handling characteristics, high flowability, and low stickiness and agglomeration (45). In the present study, the model for MC was not significant; none of the factors or interactions involved in the design had a significant effect on this response. Among others, Seville *et al.* (17) found that higher outlet temperatures led to SD powders with lower moisture contents. Nonetheless, no correlation was found between the outlet temperature and the moisture content.

As aforementioned, the highest inlet temperature used (180°C) was above the dehydrate temperature (170°C). This fact could cause a difference between the MC of the products obtained at inlet temperatures of 110°C (below the dehydrate temperature) and 180 °C (above the dehydrate temperature). Nevertheless, non-significant differences were observed, probably because the highest inlet temperature was very close to the dehydrate one.

Geometric Particle Size Distribution

The D_{50}, span, and percentage of particles below 5 μm (PPB_5) are shown in Table I for the obtained SD powders. In all cases, the span values were lower than 2, indicating that the particle size distributions were relatively narrow. As aforementioned, the particle size is a key parameter in the

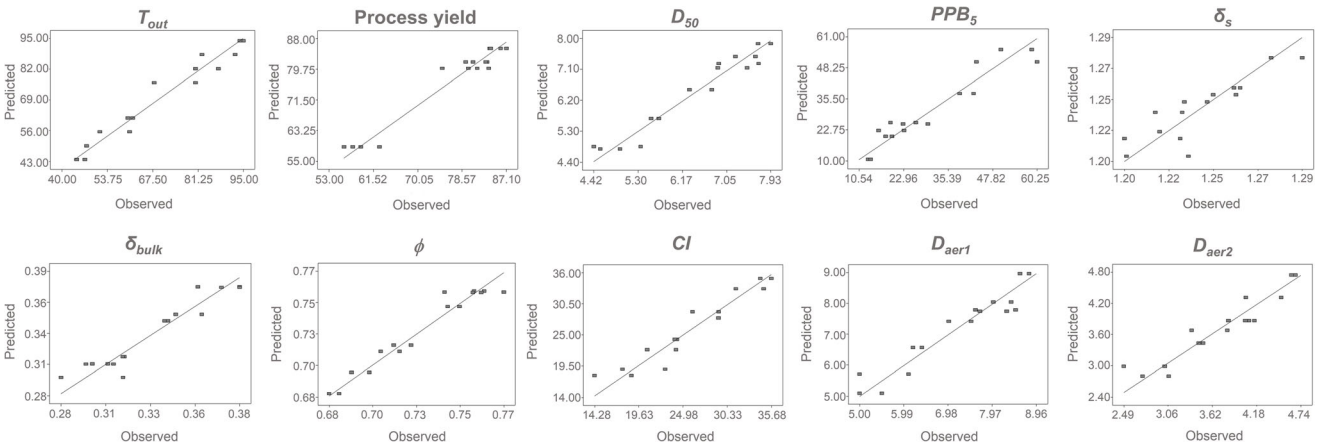

Fig. 1. Plot of the distribution of observed values *vs.* predicted values for several responses

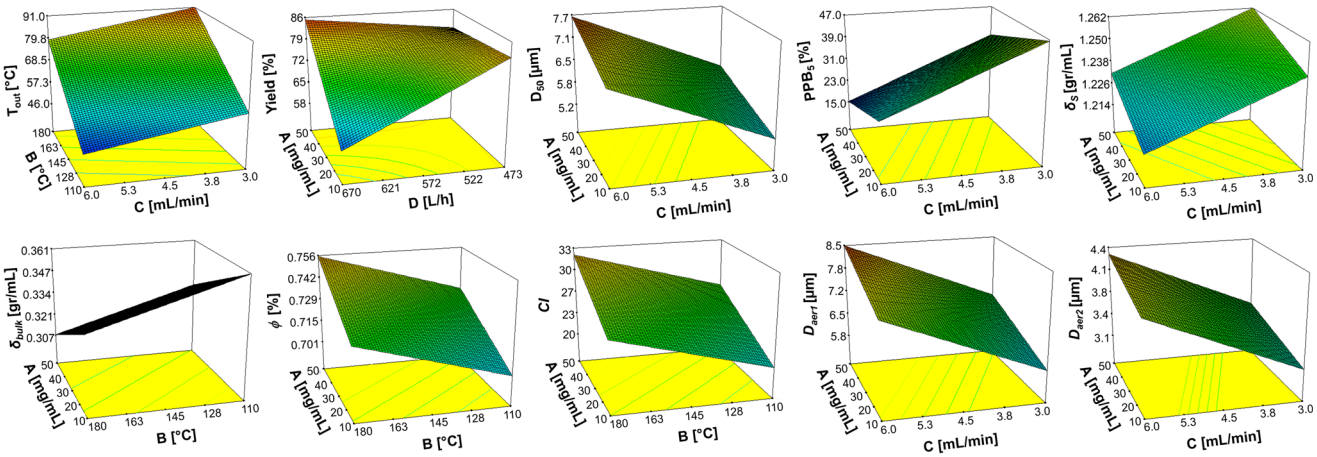

Fig. 2. Surface plot of several responses as a function of their most significant variables

optimization of a DPI formulation. None of the SD products had particles below 1 µm. Therefore, it is expected that the optimal SD product will be around the formulations with the smallest particle average size and the highest PPB_5 (*i.e.*, runs 2 and/or 10).

The fitted models for D_{50} and PPB_5 are shown in Table II. Their model p values and LOF p values indicate that these models are able to predict the corresponding responses. The high R^2 (>0.9000) and predicted R^2 (>0.700) as well as their plots of predicted value *vs.* experimental value (Fig. 1) demonstrated the goodness of their fit. For both D_{50} and PPB_5, all factors and interactions were significant, except for the AC (in D_{50}) and AB (in PPB_5) interactions. As expected, the effect of the factors is inverse for D_{50} and PPB_5 models. In both cases, the most significant factor was C (feed volumetric flow rate), followed by A (CIP concentration). Figure 2 shows the 3D plots of both responses as a function of A and C factors. As it can be seen, the D_{50} decreases and the PPB_5 increases as the CIP concentration decreases. On the other hand, the feed flow rate (C factor) had the same effect that the CIP concentration (A factor) over both D_{50} and PPB_5. These facts are in agreement with Elversson *et al.* (46) and Seville *et al.* (17). Therefore, low particle sizes are obtained using low CIP concentrations and low feed flow rates.

Skeletal, Bulk, and Tap Densities

The δ_s, δ_{bulk}, and δ_{tap} values are shown in Table I, and the fitted models corresponding to δ_s and δ_{bulk} are presented in Table II. Despite the δ_{tap} model was significant, it is not shown because its fit was very poor (*i.e.*, the R^2 and R^2 predicted were 0.5829 and 0.2584, respectively).

Figure 2 shows the effects of the most significant factors over both densities. The effect of the different factors and interactions is of the same sign on both densities (δ_s and δ_{bulk}), except for the A factor (CIP concentration) that had an opposite effect on the δ_s and δ_{bulk}. This could be explained in terms of the D_{50}. Indeed, the sign of all factors was contrary for δ_{bulk} and D_{50}. This could be due to the inverse relation between these two parameters. Bigger particles gave lower δ_{bulk} (*i.e.*, more voids between the particles) (47). For this reason, the porosity ϕ was calculated as follows (48):

$$\phi = 1 - \frac{\delta_{bulk}}{\delta_s} \tag{9}$$

The ϕ values were between 0.68 and 0.77. The corresponding ϕ values and ϕ statistical model are shown in Tables I and II, respectively. As it can be seen, the effect of factors A, B, and C had the same sign on D_{50} and ϕ (*i.e.*, the factors that increase the particle size, increase the porosity of the powder). The D factor had opposite effect on both responses, but this factor is not significant in both models.

Summarizing, an increase in the CIP concentration led to bigger particles and powders with higher porosity and, thus, with lower δ_{bulk}. On the other hand, an increase in the CIP concentration led to higher δ_s. Therefore, at higher CIP concentrations, SD products with higher particle size and density are expected.

Carr's Index

As aforementioned, Carr's index is related with the powder flowability. This index was between 14 (good flow) and 36 (very poor flow) for all the SD products. Table II shows that all factors, except for the AB and AD interactions, had a significant effect on this index. Giovagnoli *et al.* (49) reported equal effects for the spray drying of ofloxacin-Pd complexes. Figure 1 and the ANOVA results in Table II demonstrate the goodness of the model fit.

The effect of all factors in CI and D_{50} models had the same sign. Therefore, the changes that increase the particle size will decrease the powder flowability. In this sense, in the range under study the smallest particles will have the best flowability.

Estimated Aerodynamic Diameter

As aforementioned, the D_{aer1} and D_{aer2} were estimated using the δ_s and δ_{bulk}, respectively. Table I shows that D_{aer1} and D_{aer2} were in the ranges 5.0–8.8 µm and 2.5–4.7 µm, respectively. The aerodynamic diameter will be between the D_{aer1} and D_{aer2}. The corresponding fitted models are shown in Table II. The sign of all significant factors are the same in both D_{aer} and equal to the signs in the D_{50} model, being their 3D plots almost equal

(Fig. 2). Furthermore, the effects of the factors are not in all cases in agreement with the effects of the factors on δ_s and δ_{bulk}. Therefore, and according to Eqs. (3) and (4), D_{50} had a higher effect on the estimated D_{aer} than the densities.

Optimal Formulation and Operating Conditions

Based on the results previously obtained, the optimal conditions were found by using the desirability tool of the Design Expert program. The desirability function allows obtaining the experimental conditions to reach, simultaneously, the optimal value for the evaluated responses. Desirability ranges from zero to one, corresponding to undesirable responses and ideal responses, respectively (50). In this sense, the criteria were to maximize process yield and PPB_5, and to minimize *Carr's index*, D_{aer1}, and D_{aer2}. The purpose was to find a formulation with the lowest D_{aer} and D_{50}, and high percentage of particles able to access the lung. A lower CI is preferred, *i.e.*, a less compressible powder and with good flow properties.

Table III shows the set with the highest desirability (*solution 1*, 0.877). The optimal conditions correspond to the lowest A, B, C, and D factors, and runs 6 and 10 of the design. The estimated process yield is 81.6%, within the highest obtained. The estimated CI value is 18, being considered *fair* by the USP (34). Regarding the particle size, the estimated D_{aer1} and D_{aer2} are close to the lowest obtained values. In this sense, 53.5% of the particles will have a particle size below 5 μm. The D_{aer1} and D_{aer2} were 5.1 μm and 2.8 μm, respectively. Therefore, the aerodynamic diameter will be between these values, with a high percentage of particles able to access the respiratory tract.

These results can also be observed in Fig. 3. The plot is a graphical representation of the three most important responses obtained for each run (*i.e.*, D_{aer2}, CI, and process yield). As it can be seen, experiments 6 and 10 (the suggested optimal conditions) are in the upper left side of the graph, stating that they have low D_{aer2} and high process yield. Moreover, the size of the corresponding spheres is small, showing that they are within the powders with the lower CI.

Figure 3 also shows that runs 2 and 8 have the highest process yield and they are within the experiments with the lower D_{aer2} of the design. However, their CI is higher than in runs 6 and 10. The *solution 2* shown in Table III is the other suggested optimal set; the corresponding values are almost equal to the ones used in runs 2 and 8. Despite the process yield is higher than in *solution 1*, the other responses are worse. These changes are minor except for CI, which goes from fair flow (16–20) in *solution 1* to passable flow (21–25) in *solution 2*. As it can be seen in Table III, in both cases, the recommendation is to use low inlet temperature (B, 110°C) and low feed volumetric flow rate (C, 3 mL/min). On the other side, in *solution 1*, the CIP concentration and the atomization air volumetric flow rate are low (A, 10 mg/mL and D, 473 L/h), these values being the opposite for *solution 2*. Therefore, when a high CIP concentration is used, the atomization air volumetric flow rate needs to be raise, and *vice versa*. As the purpose of this article is to obtain the best CIP DPI product, the optimal conditions recommended are the ones corresponding to *solution 1*.

SEM, PXRD, and Aerosolization Performance of the Optimal SD Product

Figure 4 shows the SEM micrographs of the raw CIP powder and the product corresponding to the optimal conditions of the experimental design. As it can be seen, the SD product consists of round and dimpled particles. According to Verinhg (51), a spherical shell may be formed during drop drying that could collapse depending on the shell mechanical properties. Particle shape is relevant in DPI design. Dimpled particles have lower aerodynamic diameter than spherical particles (with similar geometrical size), increasing the possibility of reaching the deep lung (51,52). The observed shape of particles is in agreement with that reported by Lee *et al.* (28) for the spray drying of CIP aqueous solutions at different operating conditions.

It is known that spray drying could lead to the formation of the amorphous form of drug, which is less stable and more hygroscopic than the crystalline forms (53). Therefore, a PXRD analysis was carried out, principally to know if the product is crystalline or amorphous. Figure 5 shows the PXRD patterns of the raw material and the optimal SD product. As it can be seen, the positions of diffraction peaks at the 2θ axis are the same, particularly for the peaks of higher intensity. This information suggests that the crystals

Table III. Criteria for Optimization and Optimal Conditions

	Units	Goal	Lower limit	Upper limit	Solution 1	Solution 2
A	mg/mL	Is in range	10	50	10	48.2
B	°C	Is in range	110	180	110	110
C	mL/min	Is in range	3	6	3	3
D	L/h	Is in range	473	670	473	670
Yield	%	Maximize	55.9	87.1	81.6	84.1
PPB_5	%	Maximize	13.1	60.2	55.6	50.4
CI	–	Minimize	14	39	18	24
D_{aer1}	μm	Minimize	5.0	8.8	5.1	5.7
D_{aer2}	μm	Minimize	2.5	4.7	2.8	3.0
Desirability					0.877	0.757

PPB_5 percentage of particles below 5 μm, *CI* Carr's index, *D_{aer1}* aerodynamic diameter calculated with δ_s, *D_{aer2}* aerodynamic diameter calculated with δ_{bulk}

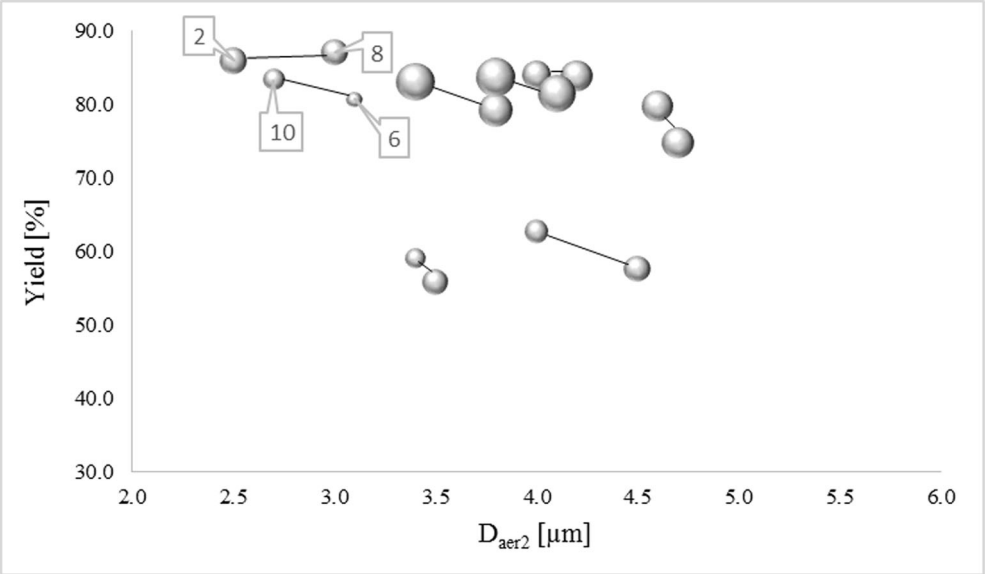

Fig. 3. Plot of the distribution of D_{aer2} *vs.* process yield. Each sphere represents a run of the design. Replicates are joined by a line. The size of the spheres is correlated with the corresponding IC

obtained for the two samples are probably of the same structure. The pattern obtained for the CIP raw material is in accordance with that reported by Liu *et al.* (43) for ciprofloxacin hydrochloride monohydrate.

As aforementioned in the "Experimental Aerodynamic Behavior" section, the aerodynamic performance of the optimal SD product was also determined. The obtained MMAD was 4.66 (± 0.05) µm, value between the D_{aer1} (5.1 µm) and D_{aer2} (2.8 µm). This result is in agreement with the fact that when the aerodynamic diameter is estimated using δ_p and δ_{bulk}, the D_{aer} is overestimated and underestimated, respectively (36). The GSD value obtained was 1.82 (± 0.02). Aerodynamic diameter distributions are considered narrow when the GSD values are below 3 (54).

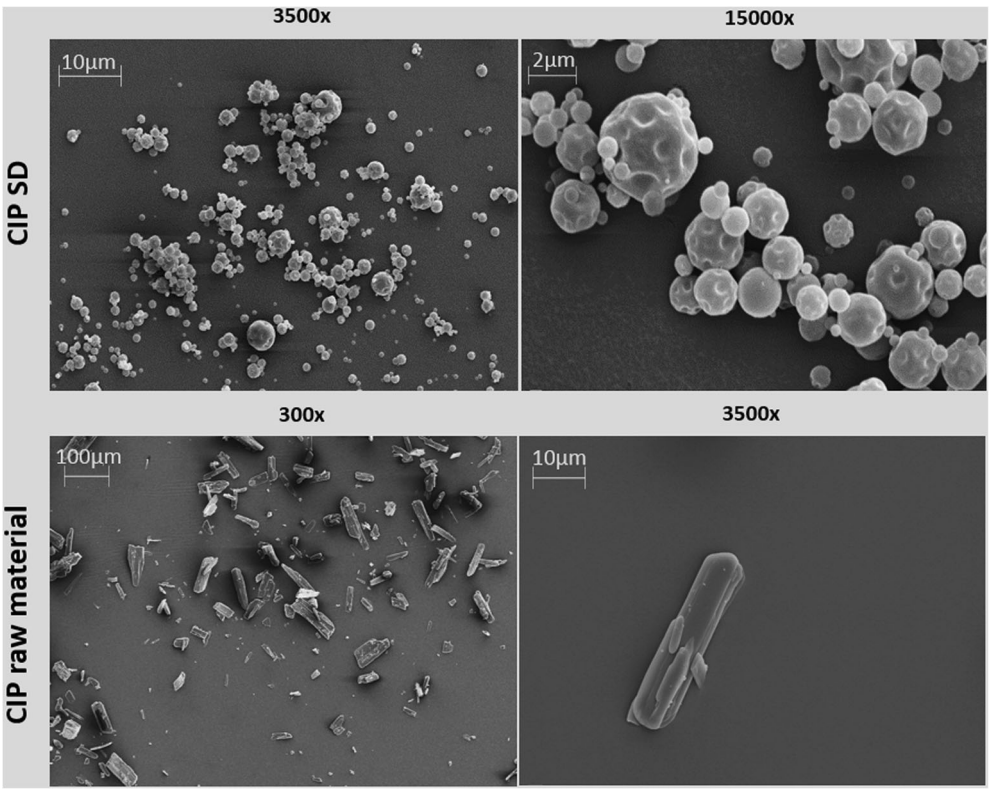

Fig. 4. Scanning electron micrographs of CIP spray-dried product (optimal point of the design) and CIP raw material

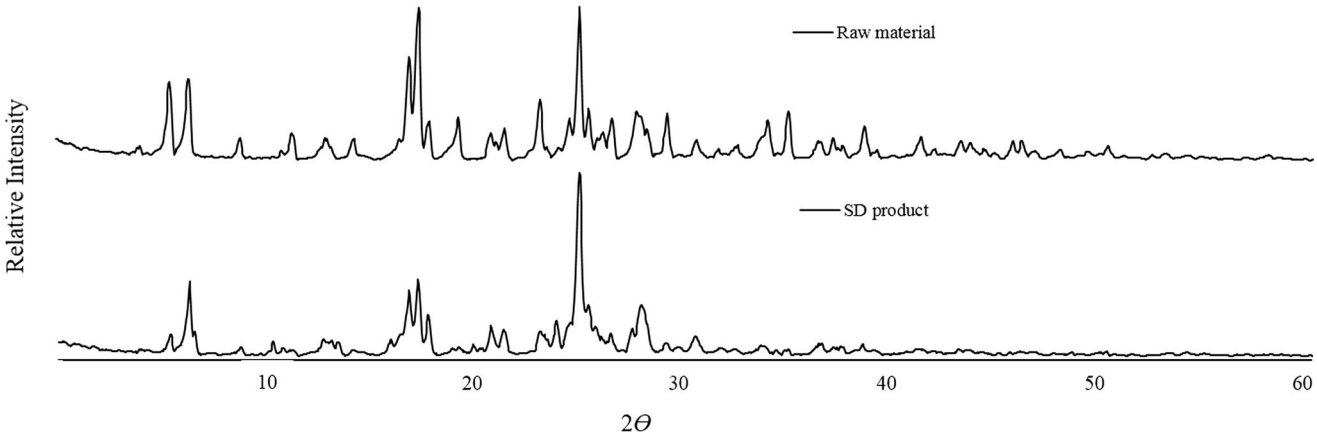

Fig. 5. PXRD diffractograms of CIP raw material and CIP spray-dried product (optimal point of the design)

Therefore, the obtained distribution can be considered narrow. The emitted fraction was 92.8 (± 0.5) %, indicating that almost all the powder leaves the device during the inhalation. On the other side, the fine particle fraction and the respirable fraction were 38.0 (± 0.1) % and 35.2 (± 0.3) %, respectively. Therefore, the results showed that more than 35% of the dose is able to access to the deep lung. In summary, the obtained aerodynamic performance (MMDA, EF, FPF, and/or RF) was improved in comparison with results previously reported (see "Comparative Study with CIP DPIs Reported in the Literature" section).

Environmental and Economic Aspects

An environmental analysis was carried out on the optimal point found in the previous section. The analysis was focused in the 12 principle of the Green Chemistry (55). The optimal point is in accordance with the first principle; *it is better to prevent waste than to treat or clean up waste after it has been created*. Indeed, a high process yield, as the one obtained, allows reducing the waste that remains stuck on the different parts of the equipment and goes to the filter as fine particles. Furthermore, scale-up of spray drying is relatively efficient and a low number of experiments would be needed to implement industrial-scale manufacturing, minimizing waste production (56).

On the other side, the fifth principle states, *the use of auxiliary substances (e.g., solvents and separation agents) should be made unnecessary wherever possible and innocuous when used*. This principle was also achieved; only water was used as solvent and no other auxiliary substance was required.

The optimal point is also in agreement with the sixth principle: *energy requirements of chemical processes should be recognized for their environmental and economic impacts and should be minimized*. Indeed, the inlet temperature was the lowest of the design. In addition, the only step required before atomization was dissolution of CIP in water, which was performed at a relatively low temperature (40°C).

The last followed principle was the twelfth one: *inherently safer chemistry for accident prevention*. In this sense, none of the raw material employed (CIP and water) produces releases, explosions, or fires, and the process was carried out at relatively low temperature and pressure. These facts are environmentally important and ensure the security of the personnel in charge of the process.

All the aforementioned principles also led to a reduction in the costs generated during the process. Indeed, high yield indicates a more efficient process, with a diminution in the amount of the required raw material. Water is the cheapest solvent. The lower energy consumption implies a reduction in the energy costs. Moreover, and due to the low risks of releases, explosions, fire, and to the personnel, the costs to prevent or repair accidents will be very low too. The production cost would be reduced by using simpler manufacturing process and formulations, which lead to more feasible large-scale programs in developing countries (57).

Comparative Study with CIP DPIs Reported in the Literature

With the purpose of showing the advantage of the present study over previous works reported in the literature, a comparative analysis of the main results is presented (13,19,23–25). Table S.II shows the used production process and the main characteristics of the developed products. As was previously mentioned in the introduction, Zhao *et al.* were the unique ones who focus their work in developing a DIP formulation containing only CIP (25). The other works presented in Table S.II have produced DPIs of CIP in combination with excipients or drugs, obtaining also DPIs containing only CIP just for comparative purposes. In those cases, the extra used components were polyvinyl alcohol, L-leucine and cyclodextrin (23), *N*-acetylcysteine and recombinant human deoxyribonuclease I (24), doxycycline (13), and mannitol (19).

In comparison with most of the current open literature, the present approach is more friendly with the environment and simpler. In this sense, some authors proposed the use of organic solvents (*e.g.*, isopropyl alcohol and ethanol) and/or additional steps previous to the SD process, such as humid ball milling, liquid anti-solvent precipitation, and homogenization. The use of more steps in the production process could result in higher energy consumption and lower yield, due to losses of material in each step. In this sense, our work and the

one carried out by Adi *et al.* (who studied co-processed materials based on polyvinyl alcohol and another antibiotic) were unique that have produced CIP powders using only spray drying and water as solvent (13–19).

As it can be seen in Table S.II, the state of the obtained products is crystalline only for the production processes that involve the use of previous step to the spray drying (24,25), while amorphous products were obtained for the cases where only a simple spray drying was carried out (13,19,23). As it was aforementioned, the crystalline state is more stable and less hygroscopic than the amorphous state (53). Regarding the process yield, Karimi *et al.* (23) were the unique ones who reported the obtained SD process yield (60–70%), which is lower than the yield determined in the present work (81.6%). For this reason, the set of optimized operating conditions proposed in this work has the advantage of producing a crystalline powder of CIP using a one-step technique with an excellent yield.

An analysis of the aerodynamic particle size is also showed in Table S.II. It is important to note that none of the other works used the impactor employed in the present article. In addition, other types of inhaler devices were used in some studies. However, the purpose is to carry out a general comparison. The MMAD and the fine particle fraction were improved with respect to all works, except for Cayli *et al.* (24). However, in that article, the emitted dose (54%) is much lower than the one obtained reported here (93%). As it can be concluded from the results reported in Table S.II, the present work has several advantages in terms of green and economic aspects, as well as in terms of the product quality.

CONCLUSION

The use of design of experiments allowed obtaining an optimal CIP SD product to be administrated in the lung as a DPI. This product has a particle size that guarantees access to the lung, moisture content acceptable for DPI, and *fair* flowability. According to the PDRX analysis, the SD product has a crystalline structure and consists of round and dimpled particles.

Moreover, the product was obtained by an easy dissolution step followed by the SD process. The only solvent used was water and no auxiliary substance or excipient was required. The process yield was high (81.5%). These characteristics, among others, make the process a green and economic production process.

ACKNOWLEDGEMENTS

The authors thank Lic. F. Cabrera and Dra. A. Di Battista (PLAPIQUI) for their technical assistance and Plastiape (Italy) for kindly supplying the RS01 inhaler device.

FUNDING INFORMATION

Financial support was received from CONICET (PIP 112-2011-0100336112), UNS (PGI 24/B209, PGI 24/M122), and FONCyT (PICT-2014-2421). M. Razuc received financial support from CONICET for her postdoctoral fellowship.

REFERENCES

1. Siddiqi A, Sethi S. Optimizing antibiotic selection in treating COPD exacerbations. Int J Chron Obstruct Pulmon Dis. 2008;3:31–44.
2. WHO. World Health Organization. Chronic respiratory diseases. Chronic obstructive pulmonary disease (COPD). http://www.who.int/respiratory/copd/en/ (Accessed 19 September 2017).
3. Sethi S, Murphy T. Bacterial infection in chronic obstructive pulmonary disease in 2000. Clin Microbiol Rev. 2001;14:336–63.
4. Emerson J, Rosenfeld M, McNamara S, Ramsey B, Gibson R. Pseudomonas aeruginosa and other predictors of mortality and morbidity in young children with cystic fibrosis. Pediatr Pulmonol. 2002;34:91–100.
5. Döring G, Flume P, Heijerman H, Elborn J. Treatment of lung infection in patients with cystic fibrosis: current and future strategies. J Cyst Fibros. 2012;11:461–79.
6. Eller J, Ede A, Schaberg T, Niederman M, Mauch H, Lode H. Infective exacerbations of chronic bronchitis: relation between bacteriologic etiology and lung function. Chest. 1998;113:1542–8.
7. Redmond A, Sweeney L, Macfarland M, Mitchell M, Daggett S, Kubin R. Oral ciprofloxacin in the treatment of pseudomonas exacerbations of pediatric cystic fibrosis: clinical efficacy and safety evaluation using magnetic resonance image scanning. J Int Med Res. 1998;26:304–12.
8. WHO, World Health Organization. Model formulary. 2008. http://apps.who.int/iris/handle/10665/44053 (Accessed 19 Sept 2017).
9. Kontou P, Chatzika K, Pitsiou G, Stanopoulos I, Argyropoulou-Pataka P, Kioumis I. Pharmacokinetics of ciprofloxacin and its penetration into bronchial secretions of mechanically ventilated patients with chronic obstructive pulmonary disease. Antimicrob Agents Chemother. 2011;55:4149–53.
10. Cipolla D. Will pulmonary drug delivery for systemic application ever fulfill its rich promise? Expert Opin Drug Deliv. 2016;13:1337–40.
11. Dimer F, de Souza Carvalho-Wodarz C, Haupenthal J, Hartmann R, Lehr C. Inhalable clarithromycin microparticles for treatment of respiratory infections. Pharm Res. 2015;32:3850–61.
12. Devarajan P, Jain S. Targeted drug delivery: concepts and design. New York: Springer; 2015. p. 22–3.
13. Adi H, Young P, Chan H, Stewart P, Agus H, Traini D. Cospray dried antibiotics for dry powder lung delivery. J Pharm Sci. 2008;97:3356–66.
14. Pilcer G, De Bueger V, Traina K, Traore H, Sebti T, Vanderbist F, et al. Carrier-free combination for dry powder inhalation of antibiotics in the treatment of lung infections in cystic fibrosis. Int J Pharm. 2013;451:112–20.
15. Alagusundaram M, Deepthi N, Ramkanth S, Angalaparameswari S, Saleem T, Gnanaprakash T, et al. Dry powder inhalers - an overview. Int J Res Pharm Sci. 2010;1:34–42.
16. Sosnik A, Seremeta K. Advantages and challenges of the spray-drying technology for the production of pure drug particles and drug-loaded polymeric carriers. Adv Colloid Interf Sci. 2015;223:40–54.
17. Seville P, Li H, Learoyd T. Spray-dried powders for pulmonary drug delivery. Crit Rev Ther Drug Carrier Syst. 2007;24:307–60.
18. Vicente J, Pinto J, Menezes J, Gaspar F. Fundamental analysis of particle formation in spray drying. Powder Technol. 2013;247:1–7.
19. Adi H, Young P, Chan H, Agus H, Traini D. Co-spray-dried mannitol–ciprofloxacin dry powder inhaler formulation for cystic fibrosis and chronic obstructive pulmonary disease. Eur J Pharm Sci. 2010;40:239–47.
20. Osman R, Kan P, Awad G, Mortada N, EL-Shamy A, Alpar O. Spray dried inhalable ciprofloxacin powder with improved aerosolisation and antimicrobial activity. Int J Pharm. 2013;449:44–58.

21. Yang Y, Tsifansky M, Shin S, Lin Q, Yeo Y. Mannitol-guided delivery of ciprofloxacin in artificial cystic fibrosis mucus model. Biotechnol Bioeng. 2011;108:1441–9.
22. Ely L, Roa W, Finlay W, Lobenberg R. Effervescent dry powder for respiratory drug delivery. Eur J Pharm Biopharm. 2007;65:346–53.
23. Karimi K, Pallagi E, Szabó-Révész P, Csóka I, Ambrus R. Development of a microparticle-based dry powder inhalation formulation of ciprofloxacin hydrochloride applying the quality by design approach. Drug Des Dev Ther. 2016;10:3331–43.
24. Cayli Y, Sahin S, Buttini F, Balducci A, Montanari A, Vural I, et al. Dry powders for the inhalation of ciprofloxacin or levofloxacin combined with a mucolytic agent for cystic fibrosis patients. Drug Dev Ind Pharm. 2017;43:1378–89.
25. Zhao H, Le Y, Liu H, Hu T, Shen Z, Yun J, et al. Preparation of microsized spherical aggregates of ultrafine ciprofloxacin particles for dry powder inhalation (DPI). Powder Technol. 2009;194:81–6.
26. Cotabarren I, Bertín D, Razuc M, Ramírez-Rigo M, Piña J. Modelling of the spray drying process for particle design. Chem Eng Res Des. 2018;132:1091–104.
27. Adi H, Young P, Chan H, Salama R, Traini D. Controlled release antibiotics for dry powder lung delivery. Drug Dev Ind Pharm. 2010;36:119–26.
28. Lee SH, Teo J, Heng D, Zhao Y, Kiong W, Ng H, et al. A novel inhaled multi-pronged attack against respiratory bacteria. Eur J Pharm Sci. 2015;70:37–44.
29. ACS-GCIPR. American Chemical Society, Green Chemistry Institute, Pharmaceutical Roundtable. https://www.acs.org/content/acs/en/greenchemistry/industry-business/pharmaceutical.html. (Accessed 19 Sept 2017).
30. Paluch K, McCabe T, Müller-Bunz H, Corrigan O, Healy A, Tajber L. Formation and physicochemical properties of crystalline and amorphous salts with different stoichiometries formed between ciprofloxacin and succinic acid. Mol Pharm. 2013;10:3640–54.
31. Gallo L, Llabot J, Allemandi D, Bucalá V, Piña J. Influence of spray-drying operating conditions on Rhamnus purshiana (Cáscara sagrada) extract powder physical properties. Powder Technol. 2011;208:205–14.
32. Anderson M, Whitcomb P. DOE Simplified. Practical tool for effective experimentation. 3rd ed. New York: CRC Press; 2007.
33. Ceschan N, Bucalá V, Ramírez-Rigo M. New alginic acid-atenolol microparticles for inhalatory drug targeting. Mater Sci Eng. 2014;41:255–66.
34. USP. United States Pharmacopeia and National Formulary. Rockville. MD. 2007. (USP 30-NF 25).
35. Ceschan N. Development of particles for inhalation administration based on polyelectrolyte-drug systems (Doctoral dissertation). 2017. http://repositoriodigital.uns.edu.ar/handle/123456789/3437 (Accessed 19 Sept 2017).
36. Wang H, John W. Particle density correction for the aerodynamic particle sizer. Aerosol Sci Technol. 1987;6:191–8.
37. Copley Scientific Ltd. Quality solutions for inhaler testing. Nottingham, UK 2015. http://www.copleyscientific.com/files/ww/brochures/Inhaler%20Testing%20Brochure%202015_Rev4_Low%20Res. (Accessed 19 Sept 2017).
38. Stass H, Nagelschmitz J, Willmann S, Delesen S, Gupta A, Baumann S. Inhalation of a dry powder ciprofloxacin formulation in healthy subjects: a phase I study. Clin Drug Investig. 2013;33:419–27.
39. De Soyza A, Aksamit T, Bandel T, Criollo M, Elborn J, Krahn U, et al. Late-breaking abstract: respire 1: ciprofloxacin DPI 32.5mg b.d. administered 14 day on/off or 28 day on/off vs placebo for 48 weeks in subjects with non-cystic fibrosis bronchiectasis (NCFB). Eur Respir J. 2016;48:272.
40. Marple V, Olson B, Santhanakrishnan K, Mitchell J, Murray S, Hudson-Curtis B. Next generation pharmaceutical impactor part II: archival calibration. J Aerosol Med. 2003;16:301–24.
41. Gallo L, Bucalá V, Ramírez-Rigo M. Formulation and characterization of polysaccharide microparticles for pulmonary delivery of sodium cromoglycate. AAPS PharmSciTech. 2017;18:1634–45.
42. Stahl K, Claesson M, Lilliehorn P, Linden H, Backstrom K. The effect of process variables on the degradation and physical properties of spray dried insulin intended for inhalation. Int J Pharm. 2002;233:227–37.
43. Liu Y, Wang J, Yin Q. The crystal habit of ciprofloxacin hydrochloride monohydrate crystal. J Cryst Growth. 2005;276:237–42.
44. Turel I, Bukovec P. Comparison of the thermal stability of ciprofloxacin and its compounds. Thermochim Acta. 1996;287:311–8.
45. Behboudi-Jobbehdar S, Soukoulis C, Yonekura L, Fisk I. Optimization of spray-drying process conditions for the production of maximally viable microencapsulated L. acidophilus NCIMB 701748. Dry Technol. 2013;31:1274–83.
46. Elversson J, Millqvist-Fureby A, Alderborn G, Elofsson U. Droplet and particle size relationship and shell thickness of inhalable lactose particles during spray drying. J Pharm Sci. 2003;92:900–10.
47. Tontul I, Topuz A. Spray-drying of fruit and vegetable juices: effect of drying conditions on the product yield and physical properties. Trends Food Sci Technol. 2017;63:91–102.
48. Nimmo J. Porosity and pore size distribution. In: Hillel D, editor. Encyclopedia of soils in the environment. London: Elsevier; 2003. p. 295–303.
49. Giovagnoli S, Palazzo F, Di Michele A, Schoubben A, Blasi P, Ricci M. The influence of feedstock and process variables on the encapsulation of drug suspensions by spray-drying in fast drying regime: the case of novel antitubercular drug–palladium complex containing polymeric microparticles. J Pharm Sci. 2014;103:1255–68.
50. Candioti L, De Zan M, Cámara M, Goicoechea H. Experimental design and multiple response optimization. Using the desirability function in analytical methods development. Talanta. 2014;124:123–38.
51. Vehring R. Pharmaceutical particle engineering via spray drying. Pharm Res. 2008;25:999–1022.
52. Robinson S, Stewart Smith S. 2005. Formulation for inhalation. US 6,926,908 B2. 09-12-2005.
53. Vippaguntaa S, Brittainb H, Granta D. Crystalline solids. Adv Drug Deliv Rev. 2001;48:3–26.
54. Razavi Rohani S, Abnous K, Tafaghodi M. Preparation and characterization of spray-dried powders intended for pulmonary delivery of insulin with regard to the selection of excipients. Int J Pharm. 2014;465:464–78.
55. Anastas P, Kirchhoff M. Origins, current status, and future challenges of green chemistry. Acc Chem Res. 2002;35:686–94.
56. McCray S and Lyon D. Green drug delivery formulations, Chapter 23 in Green techniques for organic chemistry and medicinal chemistry, W. Zhang and B.W. Cue Jr. (ed.). John Wiley & Sons, New York. 2012.
57. Hoppentocht M, Hagedoorn P, Frijlink H, de Boer A. Technological and practical challenges of dry powder inhalers and formulations. Adv Drug Deliv Rev. 2014;75:18–31.